Macromolecules

ARTICLE

pubs.acs.org/Macromolecules

Divergent Shear Thinning and Shear Thickening Behavior of Supramolecular Polymer Networks in Semidilute Entangled Polymer Solutions

Donghua Xu,[†] Chen-Yang Liu,[‡] and Stephen L. Craig*[,†]

[†]Department of Chemistry and Center for Biologically Inspired Materials and Material Systems, Duke University, Durham, North Carolina 27708-0346, United States

[‡]CAS Key Laboratory of Engineering Plastics, Joint Laboratory of Polymer Science and Materials, Institute of Chemistry, Chinese Academy of Sciences, Beijing 100190, P. R. China

Supporting Information

ABSTRACT: The steady shear behavior of metallo-supramolecular polymer networks formed by bis-Pd(II) cross-linkers and semidilute entangled solutions of poly(4-vinylpyridine) (PVP) in dimethyl sulfoxide (DMSO) or *N*,*N*-dimethylformamide (DMF) is reported. The steady shear behavior of the networks depends on the dissociation rate and association rate of the cross-linkers, the concentration of cross-linkers, and the concentration of the polymer solution. The divergent steady shear behavior—shear thinning versus shear thickening—of samples with identical structure but different cross-linker dynamics [J. Phys. Chem. Lett. 2010, 1, 1683−1686] is further explored in this paper. The divergent steady shear behavior for networks with different cross-linkers is connected to a competition between different time scales: the average time that a cross-linker remains open (τ_1) and the local relaxation time of a segment of polymer chain ($\tau_{segment}$). When τ_1 is larger than $\tau_{segment}$, shear thickening is observed. When τ_1 is smaller than $\tau_{segment}$, only shear thinning is observed.

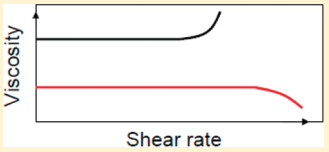

INTRODUCTION

The rich rheological behavior of associative polymers fuels their use in a wide range of applications, including rheology modifiers for paintings, cosmetics, pharmaceutics, and coatings.[1,2] Their non-Newtonian rheological behavior, e.g., shear thickening and/or shear thinning, is often at the foundation of their utility, and extensive experimental and theoretical effort has been devoted to understanding the molecular origin of shear thickening or shear thinning.[3−7]

The majority of these investigations have been performed in the semidilute unentangled regime.[8−11] While a comprehensive molecular picture remains elusive, the theories associated with shear thickening and shear thinning in this concentration regime are typically united in that they are interpreted through the time scale of a single dynamic process—the dissociation of the transient, associative cross-linkers.[3−14] The situation is more complicated as the concentration of the associative polymer solution increases into the semidilute entangled regime.[15,16] For example, English et al. reported an associative polymer solution for which shear thickening at intermediate shear rate was observed below the overlap concentration, while shear thinning was observed above the overlap concentration.[15] They concluded that in the semidilute entangled regime both topological entanglements of the polymers and the kinetics of cross-linking contributed to the rheological properties. In their work,[15] however, the reversible associations were driven by hydrophobic association, and the structure and distribution of the hydrophobic aggregates could, in principle, vary with concentration, creating some ambiguity as to the contributions of nondissociative dynamics in the entangled solutions.

Our group has previously demonstrated a useful method for probing the contributions of molecular reversibility to the rheological properties of polymers.[17−20] The method takes advantage of steric effects at the *N*-alkyl positions of *N*,*C*,*N*-pincer Pd(II) and Pt(II) complexes, through which the dissociation rate of the cross-linkers can be changed by orders of magnitude independently of the association constant.[17] This methodology allows us to differentiate the influence of cross-linker kinetics from that of other dynamic processes (e.g., disentanglement of polymer chains) or structural contributions (e.g., changes in entanglement structure and/or spacing) on the rheological behavior of the supramolecular polymer networks.

We recently reported the nonlinear rheological properties of metallo-supramolecular networks formed by the reversible cross-linking of semidilute unentangled solutions of poly(4-vinylpyridine) (PVP).[20] In these unentangled networks, shear thickening at intermediate shear rate is observed above a critical shear rate under steady shear, and that critical shear rate is experimentally correlated with the dissociation rate of the cross-linkers. Because the relaxation time of the samples increases with the applied shear stress during shear thickening, the primary mechanism of shear thickening was ascribed to the shear-induced transformation of intrachain cross-linking to interchain cross-linking, rather than nonlinear high tension along polymer chains that are stretched beyond the Gaussian range.[20]

Received: January 14, 2011
Revised: February 18, 2011
Published: March 14, 2011

When the concentration of PVP increases to the semidilute entangled regime, however, the picture is more complex. For two networks with identical cross-linker density, shear thinning is observed for the network formed with the faster cross-linkers (dissociation rate $k_d \sim 1450\ s^{-1}$), while shear thickening at intermediate shear rate is observed for the network formed with the relatively slower cross-linkers ($k_d \sim 17\ s^{-1}$).[21] To the best of our knowledge, this behavior deviates not only quantitatively, but also qualitatively, from all reported models for nonlinear rheology of associative polymer networks. Here we investigate the steady shear behavior of these semidilute entangled polymer networks in greater detail, mapping out a "structure−property phase space" for the steady shear behavior and exploring the relationships between the rate of cross-link dissociation and association, and the dynamics of polymer chain in the entangled polymer networks. The additional structure−activity relationships further support a mechanism, not previously uncovered, for nonlinear steady shear behavior that involves competition between dissociation/reassociation of the cross-linkers and dynamics of polymer chain segments in semidilute entangled PVP solutions.

EXPERIMENTAL SECTION

Materials. The bis-Pd(II) cross-linkers [2,3,5,6-tetrakis{(dimethylamino)methy}phenylene-1,4-bis(palladiumtrifluoromethanesulfonate)] (**1a**) and [2,3,5,6-tetrakis{(diethylamino)methy}phenylene-1,4-bis-(palladiumtrifluoromethanesulfonate)] (**1b**) were synthesized as reported elsewhere.[22] The binding thermodynamics and exchange kinetics of the metal−pyridine interactions have been characterized previously.[18] The equilibrium association constants (K_{eq}) and dissociation rate constants (k_d) for **1a**·pyridine in DMSO at 25 °C are 29 M^{-1} and 1450 s^{-1}, respectively. K_{eq} and k_d for **1b**·pyridine in DMSO at 25 °C are 33 M^{-1} and 17 s^{-1}, respectively.[18] Dimethyl sulfoxide (DMSO), *N*,*N*-dimethylformamide (DMF), and poly(4-vinylpyridine) (PVP) with M_w of ∼60 000 as reported from producer were used as received from Aldrich. The M_n and M_w of above PVP from Aldrich have been reported to be 22 000 and 64 300 (M_w/M_n is 2.92), respectively, in the literature.[23] Rough estimates of the Kuhn length and related parameters are provided in the Supporting Information.

Sample Preparation. Samples were prepared by mixing PVP solutions with cross-linker solutions. Two different solvents, DMSO and DMF, were used. Details of sample preparation can be found in a previous paper.[20] The concentration of cross-linkers in the samples varied from 1% to 5% (ratio of Pd atoms to N atoms in the pyridine units of the PVP), all of which are above the critical concentration to form a gel (shown previously to be ∼0.8% for ∼0.10 g/mL PVP/DMSO solutions).[24] The concentration of PVP in the samples varies from ∼0.08 g/mL (semidilute unentangled regime) to ∼0.27 g/mL (semidilute entangled regime). Details regarding the concentration regimes of the PVP/DMSO solutions and PVP/DMF solutions are provided in the Supporting Information. The critical concentration of entanglement of PVP/DMSO solution is ∼0.155 g/mL at 25 °C, while it is ∼0.148 g/mL at 50 °C. The critical concentration of entanglement of PVP/DMF solution is ∼0.147 g/mL at 25 °C while it is ∼0.145 g/mL at 0 °C (Figures S1 and S2 in the Supporting Information). The average number of entanglements per polymer chain varies from 1 to 3 in ∼0.16 to ∼0.27 g/mL PVP solution (see Table S1 in Supporting Information). Concentrations are often denoted with a "∼" to reflect the slight variation between samples made with cross-linker **1a** vs **1b**; see Supporting Information for details.

Rheological Measurements. Rheological data were obtained by using an AR G2 rheometer (TA Instruments) with cone−plate geometry (diameter of 20 mm, cone angle of 2°, truncation height of 49 μm) and concentric cylinder geometry. (The concentric cylinder geometry was used only to characterize the concentration regimes of pure PVP/DMSO and PVP/DMF solutions without cross-linkers.) A solvent trap was used with the cone−plate geometry to minimize the evaporation of solvent from the samples. Strain sweep experiments were performed at a frequency of 10 rad/s (unless otherwise noted) to determine the region of linear response. Oscillatory frequency sweeps from 0.1 to 500 rad/s were carried out with appropriate strain within the linear region. Steady shear measurements were performed over a range of shear rates between 10^{-3} and $10^{3}\ s^{-1}$, although higher shear rates were occasionally employed for samples with low viscosity. Parallel superposition of oscillation onto steady shear flow was carried out at various applied stresses to explore the mechanism of the local shear thinning and/or shear thickening in semidilute entangled solutions. A detailed introduction to the parallel superposition of oscillation onto steady shear flow technique can be found in an earlier report by Tam et al.[25] Experiments were carried out at 25 °C unless otherwise noted.

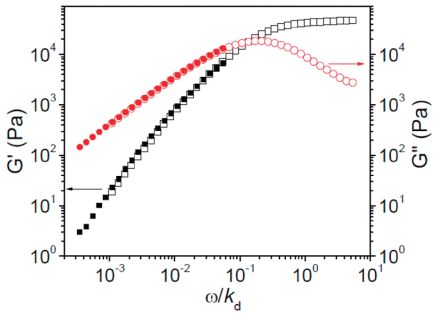

Figure 1. Storage (G') and loss (G'') moduli versus scaled frequency (ω/k_d) for ∼0.27 g/mL PVP/DMSO solution with 2% **1a** or 2% **1b**. Filled symbols represent cross-linker **1a** and unfilled symbols represent cross-linker **1b**. $T = 25$ °C. The unit for frequency (ω) here is Hz. For **1a**, $k_d = 1450\ s^{-1}$, and for **1b**, $k_d = 17\ s^{-1}$.

RESULTS

Linear Oscillatory Frequency Sweep in the Semidilute Entangled Regime. Before examining the nonlinear rheological properties of the networks, we begin by presenting the rheological properties of the network in the linear regime. In Figure 1, the linear oscillatory frequency sweep of ∼0.27 g/mL PVP/DMSO with 2% **1** is shown as an example. Although both topological entanglements between polymer chain and dissociation of cross-linkers are expected to contribute to the network relaxation, the dynamic mechanical moduli can still be superposed by the scaled frequency (oscillatory frequency divided by cross-linker dissociation rate, ω/k_d). This behavior, shown in Figure 1, is consistent with our earlier observations[20] and Leibler et al.'s theory regarding the dynamics of reversible networks.[26]

Steady Shear Results. We begin by considering networks in which the concentration of cross-linker (relative to pyridine) is held constant at 2%, but the concentration of PVP in the network is varied. The steady shear results for these networks are shown in Figure 2. At lower concentrations of the network in the semidilute unentangled regime ([PVP] < ∼0.155 g/mL), as previously reported[20] and shown again here for comparison, shear thickening at intermediate shear rate is observed for both **1a**·PVP and **1b**·PVP. At ∼ 0.16 g/mL PVP concentration (just above the critical concentration for entanglement, 0.155 g/mL),[19] modest shear thickening at intermediate shear rate is still observed for samples with either **1a** or **1b**. With the further increase of PVP

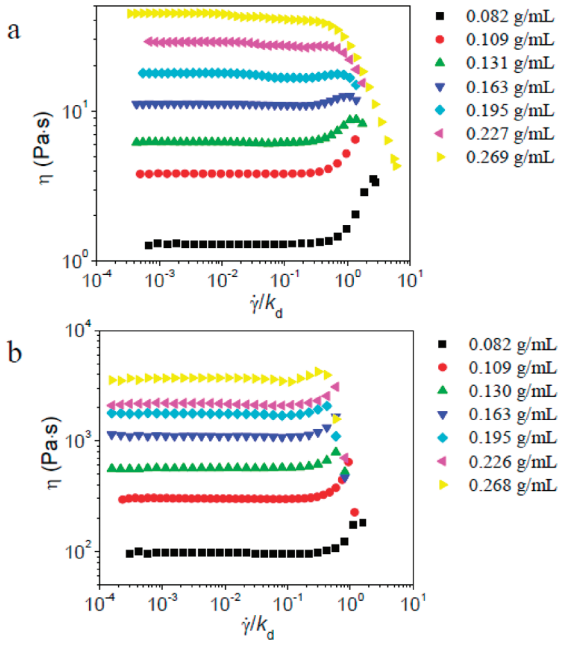

Figure 2. Steady shear viscosity (η) versus scaled shear rate ($\dot{\gamma}/k_d$) for different concentrations of PVP/DMSO solution with 2% of **1a** (a) or 2% **1b** (b) at 25 °C.[21] k_d of **1a** is 1450 s^{-1}, and k_d of **1b** is 17 s^{-1} here. Reproduced from ref 21.

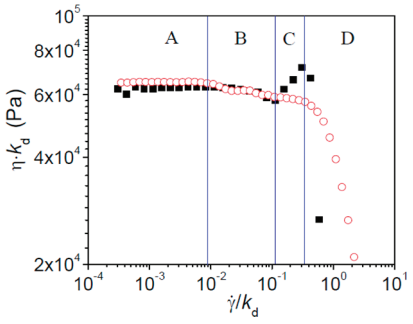

Figure 3. Scaled steady shear viscosity (ηk_d) versus scaled shear rate ($\dot{\gamma}/k_d$) for ~0.27 g/mL PVP/DMSO solutions with 2% **1a** or 2% **1b** at 25 °C. Open circles represent networks formed with cross-linker **1a**, and filled squares represent networks formed with cross-linker **1b**. For **1a**, k_d = 1450 s^{-1}, and for **1b**, k_d = 17 s^{-1}.

concentration, however, both the absolute behavior of the **1a**·PVP networks and the relative steady shear behavior of **1a**·PVP vs **1b**·PVP change. Once the PVP concentration is decidedly in the semidilute entangled regime (~0.23 and ~0.27 g/mL), samples with 2% **1a** show shear thinning, while samples with **1b** show shear thickening at intermediate shear rate.

The steady shear behavior of ~0.27 g/mL PVP/DMSO with 2% **1** is shown in greater detail in Figure 3. The steady shear viscosity of **1b**·PVP exhibits four flow regimes with increasing shear rate, which are Newtonian (regime A), local shear thinning (regime B, comprising points with a negative slope in viscosity with respect to shear rate), local shear thickening (regime C, positive slope in viscosity with respect to shear rate), and dramatic shear thinning (regime D). A curve for steady shear results of **1a**·PVP network is also divided into the four flow regimes according to the same value of scaled shear rate ($\dot{\gamma}/k_d$)

Scheme 1. Schematic Curves of Viscosity versus Shear Rate Corresponding to Four Different Classifications of Steady Shear Behavior[a]

Type	Curve of viscosity versus shear rate	Flow regimes
I		Newtonian, shear-thickening and shear-thinning
II		Newtonian, local shear thinning, local shear-thickening and shear-thinning
III		Newtonian, local shear thinning, local shear-thickening and shear-thinning
IV		Newtonian and shear-thinning

[a] Note that these classifications are qualitative only.

with **1b**·PVP network.[20] The dramatic shear thinning in regime D is attributed to network fracture and/or the subsequent ejection of sample from the rheometer geometry,[20] and it is not explored further here. In regimes A and B, the viscosities of the two samples are in inverse proportion to the relative dissociation rates of the **1a** and **1b** cross-linkers.[18,20] This is consistent with the expectation that the two samples have similar network structure in these two flow regimes, even though regime B is non-Newtonian. At the start of regime C, the Weissenberg number (the product of the shear rate and relaxation time of the network) is estimated to be 0.81 (1.93 s^{-1} × 0.42 s, sample with 2% **1b**) from the data in Figure 1. As discussed previously in our examination of rheological behavior in the semidilute unentangled regime,[20] this corresponds to the onset of polymer chain orientation. In the entangled solutions, it also corresponds to the onset of divergent behavior between the two networks; shear thinning is observed in this flow regime for **1a**·PVP, while shear thickening is observed in this flow regime for **1b**·PVP. For simplicity, we will use "shear thinning" and "shear thickening" to describe the divergent behavior of the two networks in regime C, the characteristics of which are the emphasis of this paper.

The measurements shown for 2% cross-linker concentration are repeated for samples with 1%, 3%, 4%, and 5% of **1** at different PVP/DMSO concentrations (Figures S3−S6 in Supporting Information). The remaining observed steady shear behaviors could be qualitatively classified into one of four categories shown schematically in Scheme 1, depending on the relative contributions from rate-dependent shear thinning and shear thickening. As shown in Scheme 1, type I behavior denotes a sample that transitions from Newtonian to shear-thickening behavior above a critical shear rate. Type II behavior also exhibits net shear thickening (maximum viscosity is larger than the zero shear viscosity), but there is a period of local shear thinning between the Newtonian and local shear thickening regimes. Type III behavior is similar to type II, but magnitude of the local shear thickening is not sufficient to overcome that of the local shear thinning, and so there is no net shear thickening at any shear rate. Finally, type IV behavior goes from Newtonian to shear thinning only, with no discernible region of local shear thickening.

A notable feature of the classifications in Scheme 1 is that the phenomenologically opposite behaviors of pure shear thickening and shear thinning (types I and IV) might reasonably be viewed as simply two extremes from the same continuum of behavior.

dx.doi.org/10.1021/ma2000916 |*Macromolecules* 2011, 44, 2343–2353

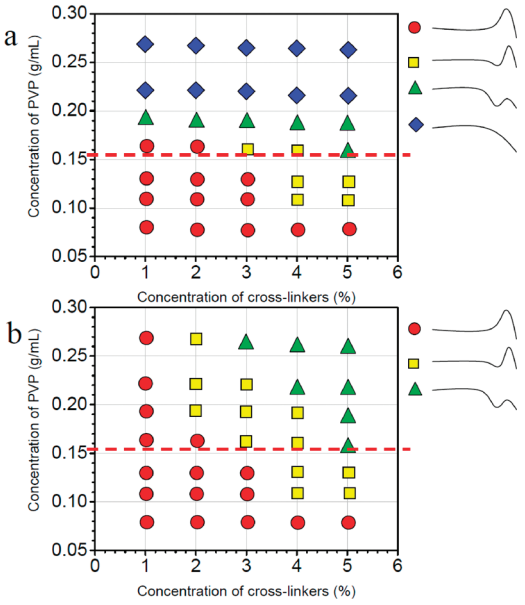

Figure 4. Steady shear behavior type (see Scheme 1) as a function of the concentration of cross-linkers and the concentration of PVP in DMSO. (a) Samples with cross-linker **1a**. (b) Samples with cross-linker **1b**. T = 25 °C. Dashed line across the chart indicates the critical concentration of entanglement (~0.155 g/mL).

Although the classification scheme itself is, *a priori*, arbitrary, the experimental results discussed below lend some credence to its validity (or, at least, its utility). The steady shear classification type is shown as a function of both the cross-linker concentration and the concentration of the PVP/DMSO solution in Figure 4. In Figure 4, four different steady shear behaviors (types I−IV in Scheme 1) are observed for samples with **1a** while only three types of steady shear behaviors (types I−III in Scheme 1) are observed for samples with **1b** in the experimental range. The steady shear behavior of the samples varies smoothly (type I borders type II, etc.), with the change of concentration of cross-linkers and concentration of PVP/DMSO solution, supporting the validity of the classification in Scheme 1. In Figure 4, the types of steady shear behavior for samples with **1a** or **1b** are the same below or just above the critical concentration of entanglement (~0.155 g/mL), whereas apparent differences are observed in Figure 4a,b with the further increase of PVP concentration. Both the concentration of cross-linkers and concentration of PVP/DMSO solution are expected to affect the fraction of interchain cross-linkers (elastically active chains),[20] and we next explore the relationship between the steady shear behavior shown in Figure 4 and the fraction of elastically active chains.

Influence of Fraction of Elastically Active Chains on Steady Shear Behavior. According to the affine network model or the phantom network model used in the unentangled polymer network and Edward's tube or related models used to describe the entangled polymer networks, the plateau modulus depends on the number density of elastically active chains (or number of entanglements).[27] For simplicity, the affine network model was used previously to calculate the apparent number density of elastically active chains (ν) in semidilute unentangled solutions,[20] and we make use of it again here. From the frequency sweep data for samples with cross-linker **1b** (Figures S7−S11 in Supporting Information), the plateau moduli (G_0) are obtained, and the apparent number density of elastically active chains (ν)

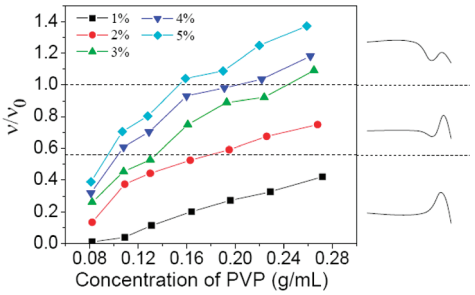

Figure 5. Fraction of elastically active chains (ν/ν_0) versus PVP concentration in DMSO for samples with different concentration of **1b**. Dashed lines are used to connect the ν/ν_0 with the steady shear behavior in Figure 4b. Types of steady shear behavior (see Scheme 1) are shown to the right of the graph for convenience. T = 25 °C.

are then calculated by the following equation[27]

$$\nu = G_0/k_B T \quad (1)$$

where k_B is Boltzmann's constant and T is the temperature. In the entangled regime, elastically active chains can result from either cross-linking or topological entanglement, and so ν is the sum of the number of interchain bound cross-linkers and entanglement knots between polymer chains. The maximum theoretical number of cross-linkers per unit volume (ν_0) in the samples is simply calculated from the concentration of cross-linkers **1a** or **1b**. We refer to the ratio of apparent to theoretical active chains, ν/ν_0, as the fraction of elastically active chains. It is apparent that the value of ν/ν_0 for some samples can be larger than 1 when topological entanglements between polymer chains contribute to the elastic modulus.[28]

Because the accessible range of frequencies is limited, it is impossible to get the G_0 of samples with cross-linkers **1a** directly, but we assume it is the same as for networks formed by **1b**. This assumption is consistent with the similar association constant of the complexes, our previous reports on similar systems,[18] and the scaling behavior observed in Figure 1. As shown in Figure 1, only the frequency (ω) is scaled by k_d of **1a** or **1b** to give the collapsed master curves. The storage (G') and loss (G'') moduli of samples with **1a** or **1b** are not scaled but are the same for a given value of scaled frequency (ω/k_d).

In Figure 5, the fraction of elastically active chains (ν/ν_0) is shown as a function of PVP concentration for samples with different concentrations of **1b**. As expected, ν/ν_0 increases with PVP/DMSO concentration, reflecting the higher probability of forming interchain bound cross-linkers at higher PVP concentration,[11] and/or topological entanglements between polymer chains contribute to the elastic modulus of samples in the semidilute entangled regime.[28] Interestingly, not only the absolute number of active cross-linkers but also ν/ν_0 increases with concentration of cross-linkers, a point not discussed further in this paper. A comparison of Figure 5 with Figure 4b shows that the three different steady shear behaviors of samples with **1b** can be related to the value of ν/ν_0, largely independently of the PVP/DMSO concentration or concentration of cross-linkers. When ν/ν_0 is smaller than ~0.6, only type I (Scheme 1) steady shear behavior is observed. For samples with a value of ν/ν_0 between ~0.6 and ~1, type II (Scheme 1) steady shear behavior is observed. When ν/ν_0 is larger than ~1, type III (Scheme 1) steady shear behavior is observed. Two dashed lines in Figure 5 separate these three regions of steady shear behavior. These

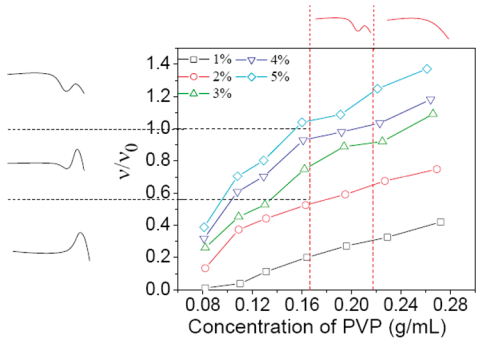

Figure 6. Fraction of elastically active chains (ν/ν_0) versus PVP concentration in DMSO for samples with different concentration of **1a**. Black dashed lines are used to connect the ν/ν_0 with the steady shear behavior in Figure 4a. Red dashed lines are used to connect the PVP concentration with the steady shear behavior in Figure 4a. Types of steady shear behavior (see Scheme 1) are shown on the perimeter of the graph for convenience. T = 25 °C.

results imply that the fractions of elastically active chains are a primary determinant of the steady shear behavior of **1b**·PVP networks.[11]

The situation, however, is more complicated for networks formed from **1a** (Figure 6). Up to just around the critical entanglement concentration (~0.16 g/mL), the type of steady shear behavior of **1a**·PVP network can be related to the value of ν/ν_0, in the same way as **1b**·PVP network. For samples in which the concentration of PVP/DMSO solution is above ~0.19 g/mL, however, the steady shear behavior of the **1a**·PVP network does not depend on ν/ν_0. Rather, it is correlated instead with the concentration of the PVP solution. When the PVP concentration is ~0.19 g/mL, samples show type III (Scheme 1) steady shear behavior. When the PVP concentration is ~0.23 or 0.27 g/mL, the networks show type IV (Scheme 1) steady shear behavior. The fact that the steady shear behavior of samples in the semidilute entanglement regime depends on the concentration of PVP suggests that physical entanglement of polymer chains have an important influence on the steady shear behavior of **1a**·PVP networks.

Changing the Dissociation Rate of Cross-Linkers by Changing Temperature. Fine-tuning of the dissociation rate is accomplished by changing the temperature. As we reported before, the k_d of **1a** and **1b** in DMSO at 50 °C is ~5400 and ~90 s^{-1}, respectively.[20] As the activation energies (E_a) for cross-link dissociation are 42 and 53 kJ/mol for **1a** and **1b**, respectively,[20] the k_d of **1a** and **1b** at 0 °C is calculated to be ~300 and ~2.4 s^{-1}, respectively, using following equation[29]

$$\ln\frac{k_2}{k_1} = \frac{E_a}{R}\left(\frac{T_2 - T_1}{T_1 T_2}\right) \qquad (2)$$

in which R is the gas constant and k_1 and k_2 are the dissociation rates at temperatures T_1 and T_2, respectively. Because DMSO freezes at 18 °C, the experiments at 0 °C were performed in DMF. This substitution is reasonable. The dynamic mechanical moduli and relaxation times of the networks in DMSO and DMF are nearly identical (Figure S14 in Supporting Information). In addition, the same divergent steady shear behavior (shear thickening at intermediate shear rate in semidilute entangled **1b**·PVP network vs shear thinning in semidilute entangled **1a**·PVP network) is observed in DMF, and the nonlinear

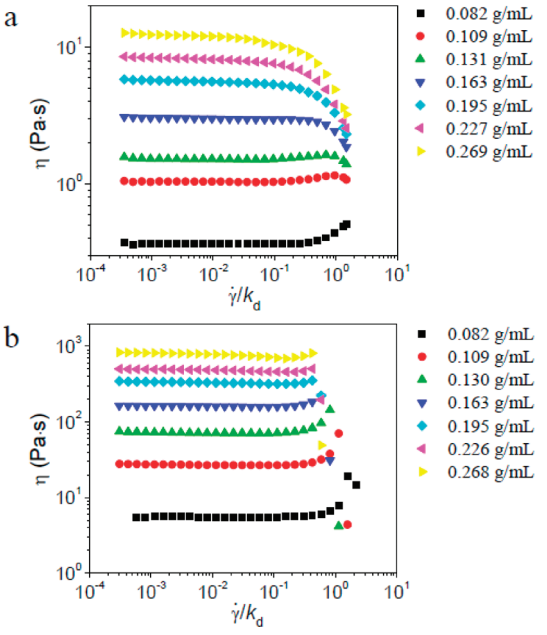

Figure 7. Steady shear viscosity (η) versus scaled shear rate ($\dot{\gamma}/k_d$) for different concentrations of PVP/DMSO solution with 2% of **1a** (a) or 2% **1b** (b) at 50 °C. Scaling is based on k_d = 5400 s^{-1} for **1a** and 90 s^{-1} for **1b**.

response starts at almost the same shear rate as in DMSO (Figure S15 in Supporting Information). We therefore conclude that both the structure of **1**·PVP network and k_d of **1** are effectively the same in DMSO and DMF.

At the same time, frequency sweep results for samples with **1b** in ~0.27 g/mL PVP solution at different temperature (Figure S16 in Supporting Information) show that the storage (G') and loss (G'') moduli of samples are the same for a given value of frequency scaled by the temperature-dependent dissociation rate (ω/k_d). We therefore infer that the topological structure (number of active cross-linkers) of the samples is similar for temperatures from 0 to 50 °C.[20]

The steady shear behavior of samples with 2% **1** at 50 °C is shown in Figure 7. When the concentration of PVP/DMSO range from ~0.16 to ~0.27 g/mL, samples with 2% **1a** all show shear thinning while samples with 2% **1b** all show shear thickening at intermediate shear rate. These data are qualitatively similar to those found at 25 °C. Also as observed at 25 °C, samples with **1a** and **1b** in the semidilute unentangled regime both show shear thickening at 50 °C.

The steady shear behavior of samples with 2% **1a** in different concentrations of PVP/DMF solution at 25 and 0 °C is shown in Figure 8. The **1b**·PVP network in PVP/DMF solution shows similar shear thickening at 0 °C that is similar to that observed at 25 °C (Figure S17, Supporting Information). In Figure 8, at 25 °C, the steady shear behavior of samples with 2% **1a** in different concentrations of PVP/DMF solution (Figure 8a) is similar to samples with 2% **1a** in PVP/DMSO solution (Figure 2a). But at 0 °C, the behavior changes. Samples with 2% **1a** at all concentrations of PVP show shear thickening at intermediate shear rate; the behavior is similar to that of **1b**·PVP network in PVP/DMSO solution (Figure 4b). The **1a**·PVP network at 0 °C is not, however, identical to the **1b**·PVP network at 25 °C; as the concentration of **1a** is increased above

dx.doi.org/10.1021/ma2000916 |*Macromolecules* 2011, 44, 2343–2353

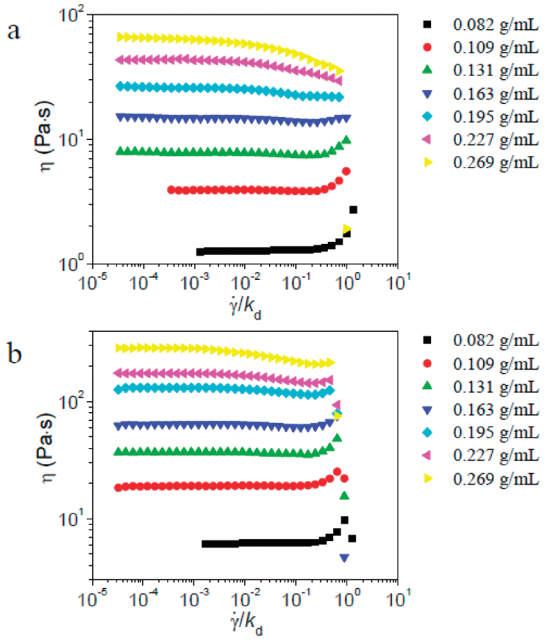

Figure 8. Steady shear viscosity (η) versus scaled shear rate ($\dot{\gamma}/k_d$) for different concentrations of PVP/DMF solution with 2% of **1a** at different temperatures. (a) 25 °C; (b) 0 °C. Scaling is based on k_d = 1450 s^{-1} for **1a** at 25 °C and 300 s^{-1} for **1a** at 0 °C.

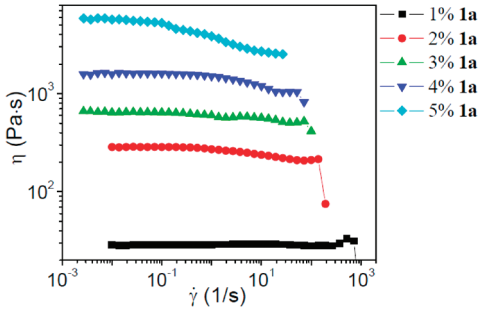

Figure 9. Steady shear viscosity (η) versus shear rate ($\dot{\gamma}$) for ~0.27 g/mL PVP/DMF solution with different concentrations of **1a** at 0 °C.

2% in ~0.27 g/mL PVP/DMF solution at 0 °C, shear thickening at intermediate shear rate is no longer observed, as shown in Figure 9. This is contrary to the results of **1b**·PVP network in PVP/DMSO solution in Figure 4b, where shear thickening at intermediate shear rate is observed for samples with 1−5% of **1b**. The reasons for this difference in behavior are discussed below.

DISCUSSION

Mechanism Underlying Local Shear Thinning. The influence of shear stress on the local shear thinning (e.g., regime B in Figure 3) is gained from studies involving parallel superposition of oscillation onto steady shear flow.[25] This technique allows us to investigate how applied shear stress (before the fracture of the network) affects the relaxation behavior of the network. This method has proven to be very useful previously in describing the balance between the disentanglement of polymer chains and the association of hydrophobic groups under steady shear.[15]

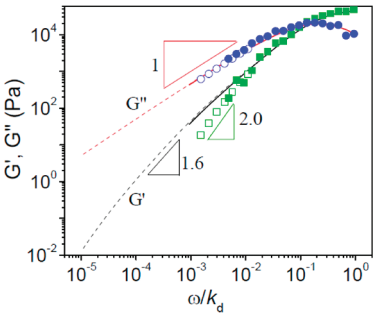

Figure 10. Storage (G') and loss (G'') moduli versus scaled frequency (ω/k_d) for ~0.27 g/mL PVP/DMSO solution with 2% of **1a** or 2% **1b** under parallel superposition of oscillation onto steady shear flow. Dashed lines and straight lines represent samples with cross-linker **1a** and **1b**, respectively, without superposed shear stress. Open symbol and filled symbols represent samples with cross-linker **1a** and **1b**, respectively, under superposed shear stress (~8000 Pa). T = 25 °C. The unit for frequency (ω) here is Hz. Scaling is based on k_d = 1450 s^{-1} for **1a** and 17 s^{-1} for **1b**.

The effects of the superposition of a steady deformation on dynamic mechanical moduli are shown in Figure 10 for ~0.27 g/mL PVP/DMSO solution with 2% **1a** or 2% **1b**. In Figure 10, the applied shear stress (~8000 Pa) is at the end point of regime B in Figure 3. The superposed shear has an apparent influence on the slope of the storage moduli (G') at low frequency; the slope of storage moduli increases from $G' \sim \omega^{1.6}$ in the absence of shear stress to $G' \sim \omega^2$ at 8000 Pa of applied shear stress. Change in the slope of the loss modulus at low frequency is not so apparent; $G'' \sim \omega^1$ both with and without applied shear stress. Similar parallel superposition of oscillation onto steady shear flow was also performed for a sample with 5% **1a** in ~0.11 g/mL PVP solution (i.e., in the semidilute unentangled regime), and a similar increase of the scaling law of G' versus frequency at low frequency is also observed in the local shear thinning regime (Figure S18, Supporting Information). This phenomenon has been referred to as a "truncation" of the relaxation spectrum, i.e., longer time modes of relaxation are lost as a consequence of the superposed shear.[15]

As noted previously, the relaxation modes in these samples are more complex than the single apparent relaxation time obtained by the crossover of G' and G''.[20] The distance between cross-linkers in the samples is not uniform, and there are different relaxation modes in the samples. A possible physical picture for the local shear thinning is depicted below. On the microscopic scale, the number of cross-linkers on each polymer chain is not the same; polymer chains with more cross-linkers have longer relaxation time. Under shear, the polymer chains with more cross-linkers deform first and induce the partial breakage of the original network structure, and some of the cross-linkers are transferred to other chains with shorter relaxation time. The final distribution of cross-linkers on each polymer chain is more homogeneous, and the relaxation mode of the samples is close to a single-element Maxwell model ($G' \sim \omega^2$ and $G'' \sim \omega^1$).[18]

Mechanisms Underlying Shear Thickening in the Semidilute Entangled Regime. How shear stress influences the structure of the network during regime C in Figure 3 was also explored by the parallel superposition of oscillation onto steady shear flow.[25] Our data are shown in Figure 11. The applied shear stress of ~8000 Pa corresponds to the starting point of regime C

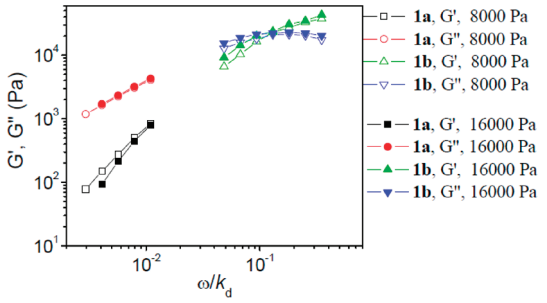

Figure 11. Storage (G') and loss (G'') moduli versus scaled frequency (ω/k_d) for ~0.27 g/mL PVP/DMSO solution with 2% of **1a** or 2% **1b** under superposed shear stress (8000 and 16 000 Pa). T = 25 °C. The unit for frequency (ω) here is Hz. k_d of **1a** is 1450 s^{-1}, and k_d of **1b** is 17 s^{-1} here.

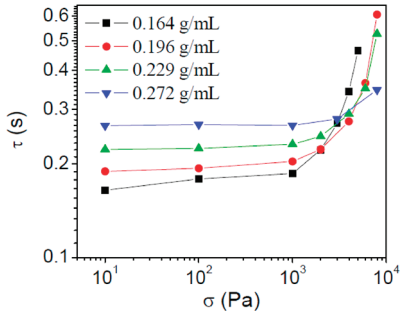

Figure 12. Plot of relaxation time (τ) of samples with 1% **1b** in different concentration of PVP/DMSO solution versus applied shear stress (σ) imposed during parallel superposition of oscillation onto steady shear flow. T = 25 °C.

(Figure 3), while the applied shear stress of ~16 000 Pa lies in the shear thickening region prior to the shear thickening maximum point (~22 000 Pa) of samples with 2% **1b**. The divergent shear thinning/thickening behavior of the **1a**·PVP vs **1b**·PVP networks is reflected in the parallel superposition experiments: as the shear stress increases from 8000 to 16 000 Pa, G' and G'' of samples with 2% **1b** both increase, while G' and G'' of samples with 2% **1a** decrease or stay roughly constant, respectively.

In Figure 11, the relaxation time (τ) of samples with 2% **1b** increases slightly from ~0.52 to ~0.55 s with increasing of shear stress from 8000 to 16 000 Pa. This is connected with the small degree of shear thickening (maximum viscosity vs zero-shear viscosity), as shown in Figure 2b.[20] Samples with 1% **1b**, however, have a larger degree of shear thickening at intermediate shear rate (Figure S3b in Supporting Information) than the samples with 2% **1b**. In Figure 12, τ of samples with 1% **1b** in semidilute entangled PVP/DMSO solution versus applied shear stress imposed during oscillation measurements are shown. To be sure that the network is not broken during the experiments, the maximum applied shear stress used is less than the critical shear stress at the shear thickening maximum point. Comparison with the steady shear data (Figure S3b in Supporting Information) shows that τ increases in the shear thickening regime. Similar behavior has been observed for samples in the semidilute unentangled regime,[20] and the results in Figure 12 support that shear thickening in the semidilute entangled PVP/DMSO solution has the same mechanism as in the semidilute unentangled regime: the shear induced conversion of intrachain cross-linkers to interchain cross-linkers.[20]

Possible Mechanisms Underlying Divergent Shear Thinning versus Shear Thickening Behavior. In considering the origins of the divergent shear thinning vs shear thickening in regime C of Figure 3, we first rule out contributions from two mechanisms that have been invoked to explain shear thinning and/or shear thickening in related systems. The first is the influence of shear stress on the dissociation of the coordinative cross-links. In Regalado et al.'s work,[16] shear thinning in the semidilute entangled regime is tentatively attributed to the change of lifetime in active cross-linkers that are coupled to the shear flow. In other words, shear thinning may be caused by an increase in the dissociation rate under applied stress.[30] Such effects are possible contributors to the observed shear thinning here. Force-accelerated dissociation of similar Pd(II)−pyridine complexes has been observed by single-molecular force spectroscopy,[31,32] and (presumably much larger) shear forces during sonication have been used to activate latent mechanocatalysts.[33] The force induced increase in dissociation, however, is expected to be very similar for cross-linkers **1a** and **1b** because of the similarity in the mechanisms of pyridine displacement.[31] The influence of stress on dissociation rate, therefore, cannot explain the divergent steady shear behavior for samples with **1a** and **1b** in semidilute entangled PVP solutions, which occur under similar applied shear stress.

Second, Tripathi et al. reported that for $C_{16}H_{33}$ end-capped urethane-coupled poly(oxyethylene) with molecular weights (M_w) of 65.3 kDa shear thickening is observed at a concentration of 20 kg/m^3 while only shear thinning is observed at a concentration of 40 kg/m^3.[11] The authors reasoned that at high concentrations the distance between neighboring micelles is small, and so there exist large numbers of active bridging chains. The flow-induced generation of active bridging chains, responsible for shear thickening at low concentrations, is therefore minimal, and only shear thinning is observed in concentrated samples.[11] Although the shear thickening observed in **1b**·PVP is attributed to the formation of new active cross-linkers; however, the fraction of elastically active chains for samples with identical concentration of **1a** and **1b** in the fixed PVP concentration is the same (Figures 5 and 6). The absence of shear thickening in **1a**·PVP, therefore, is not due to a difference in its nascent structure but instead to a difference in its dynamics.[21]

Coupling of Cross-Linker Kinetics and Polymer Chain Dynamics. The divergent steady shear behavior is only observed in the semidilute entangled regime, suggesting the influence of chain entanglement, so the nonlinear steady shear behavior in the semidilute entangled regime implies that the contribution from different time scales is that between the kinetics of cross-linkers and the dynamics of polymer chains in the semidilute entangled solution.

We discuss the kinetics of cross-linker dissociation and reassociation and the dynamics of polymer chain segments in terms of their respective time scales. The lifetime ($\tau_0 = 1/k_d$) of a cross-linker is the average time that the cross-linker spends in the closed state.[34] The average time of cross-linkers remain in the open state (τ_1, τ_1 is termed as free time of a cross-linker in later discussion) is calculated by

$$\tau_1 = 1/(k_a C_N) \quad (3)$$

where k_a is the association rate constant for cross-linker formation and C_N is the concentration of pyridine monomer. In Leibler

dx.doi.org/10.1021/ma2000916 |Macromolecules 2011, 44, 2343–2353

Table 1. Values of $\tau_0/\bar{\tau}_e$ and $\tau_1/\bar{\tau}_e$ for Samples with 1−5% of Cross-Linker 1a or 1b in 0.16−0.27 g/mL PVP/DMSO or PVP/DMF Solution at Different Temperatures[a]

		conditions			
ratio of time scales	cross-linker	PVP/DMSO, 25 °C	PVP/DMSO, 50 °C	PVP/DMF, 25 °C	PVP/DMF, 0 °C
$\tau_0/\bar{\tau}_e$	**1a**	26	30	90	*250*
	1b	**2300**	**1800**	**7600**	**32000**
$\tau_1/\bar{\tau}_e$	**1a**	0.4	0.5	1.5	*4.2*
	1b	**38**	**30**	**130**	**530**

[a] τ_0 is the lifetime of intact cross-linkers, and τ_1 is the free time of partially dissociated cross-linkers. $\bar{\tau}_e$ is the average value of the relaxation time of an entanglement strand $[\tau_e(\phi)]$ in ∼0.16 to ∼0.27 g/mL PVP/DMSO (or PVP/DMF) solution at different temperatures. Bold values indicate samples for which shear thickening is observed in ∼0.27 g/mL PVP solution with 1−5% cross-linkers, whereas unbolded values indicate samples for which shear thinning is observed in ∼0.27 g/mL PVP solution with 1−5% cross-linkers, and the italicized entry corresponds to shear thinning or shear thickening behavior in ∼0.27 g/mL PVP solution, depending on cross-linker concentration.

et al.'s work,[26] the average time of a cross-linker remains in the open state (τ_1) is given by

$$\tau_1 = \tau_0(1-p)/p \quad (4)$$

where p is the fraction of closed cross-linkers. As shown in our previous calculations regarding the fraction of closed cross-linkers (p),[20] eq 3 can be obtained from eq 4.

In eq 3, the association rate constant k_a is not measured directly but is calculated from the reported equilibrium constant for pyridine association, $K_{eq} = k_a/k_d$, which is ∼30 M^{-1}, as k_d of cross-linkers are known.[22] We acknowledge that this is an approximate value and does not account for steric or electronic contributions from tethering the pyridine to the PVP backbone.[21] Nonetheless, pyridine coordination has proven to be a useful model for pincer coordination to PVP, and the true value probably does not deviate substantially from that of the model system.[18] The concentration of pyridine monomer (C_N) in eq 3 is calculated from the concentration of PVP solution. We should note that the true value of the free time of a cross-linker (τ_1) in the network depends on the local concentration of pyridine monomer $[C_N(\text{local})]$ rather than the overall concentration of pyridine monomer (C_N) in the PVP solution. However, because $C_N(\text{local})$ cannot be determined experimentally, the whole concentration of pyridine monomer (C_N) in the PVP solution is used to calculate τ_1. As the concentration of pyridine monomer (C_N) ranges from 1.5 to 2.6 M in ∼0.16 to ∼0.27 g/mL PVP solution, we use the average value of $C_N = 2$ M to obtain $\tau_1 = \tau_0/60$.

In order to characterize the intrinsic dynamics of the polymer chains, the disentanglement times (τ_d) of pure semidilute entangled PVP/DMSO (or PVP/DMF) solutions were determined in the absence of cross-linker, by identifying the shear rate at the onset of shear thinning at different concentrations (Figures S19 and S20, Supporting Information). Shear thinning occurs in semidilute entangled solutions as polymer chains disentangle under conditions in which when the Weissenberg number is larger than 1, giving τ_d.[35,36] The Rouse relaxation time of a chain of length equal to one tube segment $[\tau_e(\phi)]$ as a function of concentration is then calculated from the value of τ_d (see Supporting Information).[27,37] Relative to the uncertainties discussed above, the resulting $\tau_e(\phi)$ does not change substantially from ∼0.16 to ∼0.27 g/mL (Figure S21, Supporting Information), and so $\bar{\tau}_e$—an average value of $\tau_e(\phi)$ for PVP concentrations of from ∼0.16 to ∼0.27 g/mL—is used to represent the dynamics of the polymer chains in PVP/DMSO (or PVP/DMF) at different temperature. This does not mean, however, that the concentration of PVP does not affect the critical polymer dynamics but simply that attempts to assign a precise value to $\tau_e(\phi)$ are unwarranted. We will return to the influence of concentration on $\tau_e(\phi)$ later.

For samples with from 1% to 5% of **1a** or **1b** in 0.16−0.27 g/mL PVP/DMSO or PVP/DMF solution at different temperatures, the average distance between two cross-linkers (r) along the polymer chain is smaller than the tube diameter (a)[27] in the semidilute entangled regime, and most r are larger than the correlation length (ξ)[27] in the semidilute entangled regime (Supporting Information). For this reason, a discussion in terms of $\bar{\tau}_e$ is more appropriate than τ_d.[27] Though the dynamics of free polymer chain segments in the cross-linked networks should differ from the dynamics of polymer chains in pure PVP solution,[26] $\bar{\tau}_e$ provides a useful metric for discussing the critical competition between dynamic time scales.

A quantitative comparison of the different time scales in various samples is provided in Figures S22−S25, and results in the semidilute entangled regime are summarized in Table 1. As discussed previously, the mechanism of shear thickening involves shear induced conversion of intrachain cross-linking to interchain cross-linking.[20] The microscopic physical picture is that the intrachain cross-linkers break first, then the polymer chain is oriented and reorganized under shear, and finally the cross-linkers recombine between two different chains. The average time from cross-linker dissociation to recombination is given by τ_1. For the polymer chain, the local orientation and reorganization of a polymer chain segment are connected to its ability to diffuse within the remainder of an intact network, and the time scale of this diffusion, dubbed here $\tau_{segment}$, is roughly estimated by the value of $\bar{\tau}_e$ described above. Table 1 shows that the critical competition occurs not between polymer segment relaxation and cross-linker dissociation; dissociation is always much slower than segmental motion. Rather, the important balance is between polymer segment relaxation and reassociation of the cross-linker. Comparing the results in Table 1 with the steady shear behavior of samples in ∼0.27 g/mL PVP solution (the influence of concentration of PVP on steady shear behavior will be discussed below), shear thickening is observed for values of $\tau_1/\bar{\tau}_e$ that are much greater than ∼4.2, and mixed behavior (shear thinning or shear thickening, depending on cross-linker concentration) is observed for samples with values of $\tau_1/\bar{\tau}_e$ around ∼4.2, and only shear thinning is observed for values of values of $\tau_1/\bar{\tau}_e$ that are less than ∼4.2. We note that $\bar{\tau}_e$ might underestimate $\tau_{segment}$

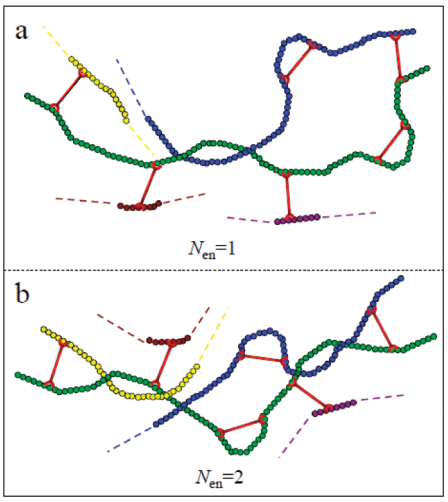

Figure 13. Schematic picture of the original **1**·PVP network with different average number of entanglements (N_{en}) per polymer chain (green). (a) N_{en} is one; (b) N_{en} is two.

because $\tau_{segment}$ is the time scale of local motions in the network, while $\bar{\tau}_e$ is extrapolated from the shear thinning data in pure semidilute entangled PVP solution without cross-linkers. Considering the approximations necessary in our calculations of τ_1 and $\bar{\tau}_e$, we regard $\tau_1/\bar{\tau}_e \sim 4$ to correspond to conditions under which $\tau_1/\tau_{segment} \sim 1$.

The value of $\tau_1/\bar{\tau}_e$ is based on average values, and it is not the only parameter that determines the steady shear behavior of the networks: the concentration of polymer also plays a role. For the **1a**·PVP networks, for example, the value of $\tau_1/\bar{\tau}_e$ is smaller than 4.2 in semidilute entangled PVP/DMSO solution at 25 and 50 °C and in semidilute entangled PVP/DMF solution at 25 °C. For semidilute entangled PVP/DMSO solution at 50 °C, no shear thickening is observed in ∼0.16 to ∼0.27 g/mL PVP/DMSO solution, and this is consistent with the value of $\tau_1/\bar{\tau}_e$ that is smaller than ∼4.2. Shear thickening is observed, however, in ∼0.16 to ∼0.19 g/mL PVP/DMSO solutions at 25 °C (Figure 4a) and in ∼0.16 g/mL PVP/DMF solutions at 25 °C (Figure 8a). Only the samples with PVP concentration decidedly in the semidilute entangled regime (∼0.23 and ∼0.27 g/mL) exhibit purely shear thinning behavior (Figure 4a). We note here that the critical concentration for entanglement (see Figures S1 and S2 in Supporting Information) is determined by a semi-empirical method,[38,39] and it is possible that the ∼0.16 g/mL PVP/DMSO solutions at 25 °C may still be in the semidilute unentangled regime, as the inferred critical concentration for entanglement is 0.155 g/mL. The samples with **1a** in ∼0.19 g/mL PVP/DMSO solutions at 25 °C, however, exhibit steady shear behavior that is quite different from that of samples in the semidilute unentangled regime (Figure 4a), and so we believe that the ∼0.19 g/mL PVP/DMSO solutions at 25 °C are definitely in the semidilute entangled regime. As shear thickening is still observed in these samples (but not at higher PVP concentration), a value of $\tau_1/\bar{\tau}_e$ is not the full criterion for steady shear behavior in these samples. The concentration of PVP solution in the semidilute entangled regime, or microscopically, the number of entanglements per polymer chain, also influences the steady shear behavior.

The number of topological entanglements per polymer chain increases with concentration and varies for our samples from 1 to 3 for concentrations of PVP from ∼0.16 to ∼0.27 g/mL (Table S1 in Supporting Information). In Figure 13a, we depict the original **1**·PVP network in which the number of entanglements per polymer chain is only one, close to that in the ∼0.16 and ∼0.19 g/mL PVP solutions. In Figure 13b, we depict a situation in which the number of entanglements per polymer chain is two, close to that in the ∼0.23 and ∼0.27 g/mL PVP solutions. In Figure 13a,b, the total number of cross-linkers and the number of intrachain cross-linkers are fixed. In Figure 13a, as most of the intrachain cross-linkers are not constrained by the single entanglement point of the polymer chain, the local disentanglement and/or chain slippage of the polymer strand is not always necessary for the transfer of intrachain cross-linkers to interchain cross-linkers. In Figure 13a, the dynamics of a segment of PVP chain with one intrachain cross-linker are best described in this case by a relaxation time ($\tau_{segment}$) that is smaller than $\bar{\tau}_e$, so the recombination time (τ_1) of dissociated cross-linkers are larger than $\tau_{segment}$, and so the polymer segment can be oriented under shear, permitting the transfer of intrachain cross-linking to interchain cross-linking and resulting in shear thickening. This differential effect is particular to the local polymer segment dynamics in a way that is not captured in the analysis based on the ratio $\tau_1/\bar{\tau}_e$ in Table 1. This situation can be extrapolated to the semidilute unentangled regime, for which $\tau_{segment}$ is far smaller than τ_1 for both cross-linkers **1a** and **1b**, and for which shear thickening is observed in all samples.[20] In Figure 13b, with the increase of PVP concentration above ∼0.23 g/mL, the larger number of entanglements per polymer chain bracket and constrain intrachain cross-linkers, so that local disentanglement and/or chain slippage of the polymer strand is needed for orientation, and the ratio $\tau_1/\bar{\tau}_e$ in Table 1 can described the steady shear behavior in ∼0.23 and ∼0.27 g/mL PVP solutions.

The local effects of cross-linker density are similarly not fully accounted for in the simplest model. We now return to samples with 1% and 2% of **1a** in ∼0.27 g/mL PVP/DMF at 0 °C, for which shear thickening is observed (Figure 9) and for which $\tau_1/\bar{\tau}_e$ of around 4.2 placing it at the extreme of samples for which that is true (Table 1). As the concentration of **1a** increases to 3% or greater, the shear thickening disappears. On the contrary, for **1b**·PVP network in ∼0.27 g/mL PVP/DMSO solution at 25 °C (Figure 4b), shear thickening at intermediate shear rate is observed for samples with 1% to 5% of **1b**, as $\tau_1/\bar{\tau}_e$ is larger than ∼4.2 (Table 1). As the concentration of cross-linkers is increased, the number of cross-linkers in an entangled strand of polymer chain increases. When the intrachain cross-linkers open, other nearby cross-linkers remain closed, and local segmental orientation is retarded (i.e., $\tau_{segment}$ increases). The effect of multiple physical cross-linkers on chain relaxation has been discussed previously, most notably by Leibler et al.,[26] who have noted the importance of considering the dynamic interplay of multiple interactions (albeit in a different context). In ∼0.27 g/mL PVP/DMF with **1a** at 0 °C, we suggest that the increasing concentration of cross-linkers above 3% forces $\tau_{segment}$ to be greater than τ_1 and precludes the reorientation necessary for shear thickening. As with the effect of concentration of cross-linkers, the effect of additional cross-linking is only significant in situations where $\tau_{segment}$ is close to τ_1 (here, when $\tau_1/\bar{\tau}_e \sim 4$).

We therefore propose that the microscopic physical significance of the competition between τ_1 and $\tau_{segment}$ is captured in Figure 14. In Figure 14, the original local **1**·PVP network has an intrachain cross-linker in a segment of polymer chain with relaxation $\tau_{segment}$, and we assume the cross-linkers are closed

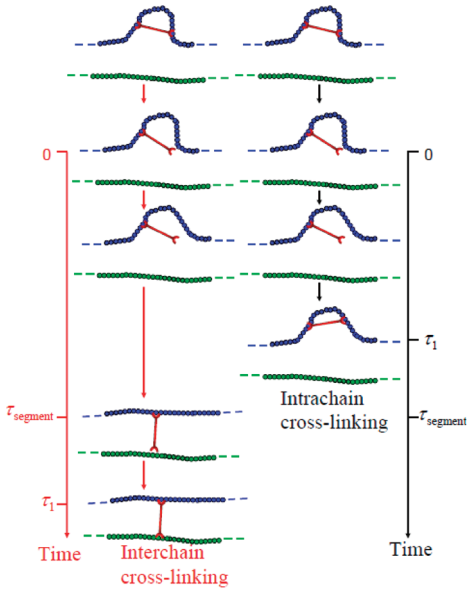

Figure 14. Schematic picture about the deformation of original local **1**·PVP network has an intrachain cross-linkers in a segment of polymer chain with relaxation $\tau_{segment}$. Left side: τ_1 is larger than $\tau_{segment}$ ($\tau_1 > \tau_{segment}$). Right side: τ_1 is smaller than $\tau_{segment}$ ($\tau_1 < \tau_{segment}$).

in the original network. The cross-linkers will open during shear deformation (at time 0 in Figure 14). When τ_1 is smaller than $\tau_{segment}$ (right side of Figure 14), the segment of polymer chain does not have enough time to slip or disentangle altogether before the cross-linker recombines after time τ_1. In this case, the lack of reorganization does not permit cross-linkers to form interchain cross-linkers, instead remaining intrachain cross-linkers, which are not elastically active. As a result, no shear thickening is observed.[19] When τ_1 is larger than $\tau_{segment}$ (left side of Figure 14), the polymer chain segment disentangles and/or slips along the entanglement and orients under shear after time $\tau_{segment}$, and recombination after time τ_1 results in the transfer from intrachain to interchain cross-linkers. Because the total number of elastically active chain increases, shear thickening results.[20] The scheme shown in Figure 14 is obviously meant to capture average ensemble behavior only, and the actual occurrence of the individual processes will, in practice, be dictated by the probabilities associated with the kinetics.

CONCLUSIONS

We have described the rich steady shear behavior of metallosupramolecular networks formed by bis-Pd(II) cross-linkers in semidilute entangled PVP solution. The mechanism behind the divergent steady shear behavior—shear thinning versus shear thickening at intermediate shear rate—for samples with different cross-linker dynamics is explored. Empirical "phase diagrams" for steady shear behavior indicate that shear thinning and shear thickening are simply different end points on a continuum of shear response, and they point to the importance of chain entanglements and the number of inactive ("intrachain") cross-linkers in the zero-shear state, the latter of which serve as latent cross-linkers that are activated as stress-bearing sites upon shear-induced network reorganization. A competition between cross-linker recombination and polymer segment orientation is implicated as the determinant of the divergent behavior observed as a function of cross-linker dynamics. Two time scales—the average time that a cross-linker remains open (τ_1) and the local relaxation time of a polymer chain segment ($\tau_{segment}$)—are used to compare the time scale of cross-linker recombination and polymer segment orientation, respectively. When τ_1 is larger than $\tau_{segment}$ ($\tau_1 > \tau_{segment}$), shear thickening is observed. When τ_1 is smaller than $\tau_{segment}$ ($\tau_1 < \tau_{segment}$), no shear thickening is observed. The criteria also apply for the steady shear behavior of samples in the semidilute unentangled regime.

ASSOCIATED CONTENT

Supporting Information. Characterization of the concentration regime of PVP/DMSO and PVP/DMF solution, steady shear and frequency sweep data, estimation of dissociation rate of cross-linkers in DMF, characterization of the disentanglement time of pure PVP/DMSO and PVP/DMF solutions, and relevant time and length scales characteristic of the samples. This material is available free of charge via the Internet at http://pubs.acs.org.

AUTHOR INFORMATION

Corresponding Author
*E-mail: stephen.craig@duke.edu.

ACKNOWLEDGMENT

S.C. thanks the NSF (CHE-0646670) and NIH (EB-001037) for financial support of this work. C.Y.L. acknowledges financial support from the National Natural Science Foundation of China (Grant 20874109). D.X. and S.C. are grateful for insightful discussions with Prof. M. Rubinstein.

REFERENCES

(1) Berret, J. F.; Calvet, D.; Collet, A.; Viguier, M. *Curr. Opin. Colloid Interface Sci.* **2003**, *8*, 296–306.
(2) Pellens, L.; Corrales, R. G.; Mewis, J. *J. Rheol.* **2004**, *48*, 379–393.
(3) Marrucci, G.; Bhargava, S.; Cooper, S. L. *Macromolecules* **1993**, *26*, 6483–6488.
(4) Indei, T. *J. Non-Newtonian Fluid Mech.* **2007**, *141*, 18–42.
(5) Wang, S. Q. *Macromolecules* **1992**, *25*, 7003–7010.
(6) Witten, T. A., Jr.; Cohen, M. H. *Macromolecules* **1985**, *18*, 1915–1918.
(7) Hoy, R. S.; Fredrickson, G. H. *J. Chem. Phys.* **2009**, *131*, 224902.
(8) Annable, T.; Buscall, R.; Ettelaie, R.; Whittlestone, D. *J. Rheol.* **1993**, *37*, 695–726.
(9) Sadeghy, K.; James, D. F. *J. Non-Newtonian Fluid Mech.* **2000**, *90*, 127–158.
(10) Berret, J. F.; Séréro, Y.; Winkelman, B.; Calvet, D.; Collet, A.; Viguier, M. *J. Rheol.* **2001**, *45*, 477–492.
(11) Tripathi, A.; Tam, K. C.; McKinley, G. H. *Macromolecules* **2006**, *39*, 1981–1999.
(12) Mewis, J.; Kaffashi, B.; Vermant, J.; Butera, R. J. *Macromolecules* **2001**, *34*, 1376–1383.
(13) Tirtaatmadja, V.; Tam, K. C.; Jenkins, R. D. *Macromolecules* **1997**, *30*, 1426–1433.
(14) Ma, S. X.; Cooper, S. L. *Macromolecules* **2001**, *34*, 3294–3301.
(15) English, R. J.; Gulati, H. S.; Jenkins, R. D.; Khan, S. A. *J. Rheol.* **1997**, *41*, 427–444.
(16) Regalado, E. J.; Joseph Selb, J.; Candau, F. *Macromolecules* **1999**, *32*, 8580–8588.
(17) Yount, W. C.; Juwarker, H.; Craig, S. L. *J. Am. Chem. Soc.* **2003**, *125*, 15302–15303.

(18) Yount, W. C.; Loveless, D. M.; Craig, S. L. *J. Am. Chem. Soc.* **2005**, *127*, 14488–14496.
(19) Loveless, D. M.; Jeon, S. L.; Craig, S. L. *Macromolecules* **2005**, *38*, 10171–10177.
(20) Xu, D.; Hawk, J.; Loveless, D. M.; Jeon, S. L.; Craig, S. L. *Macromolecules* **2010**, *43*, 3556–3565.
(21) Xu, D.; Craig, S. L. *J. Phys. Chem. Lett.* **2010**, *1*, 1683–1686.
(22) Jeon, S. L.; Loveless, D. M.; Yount, W. C.; Craig, S. L. *Inorg. Chem.* **2006**, *45*, 11060–11068.
(23) Chen, D.; Handa, H.; Wan, L.; Mao, G. *Macromol. Rapid Commun.* **2007**, *28*, 1619–1623.
(24) Loveless, D. M.; Jeon, S. L.; Craig, S. L. *J. Mater. Chem.* **2007**, *17*, 56–61.
(25) Tam, K. C.; Jenkins, R. D.; Winnik, M. A.; Bassett, D. R. *Macromolecules* **1998**, *31*, 4149–4159.
(26) Leibler, L.; Rubinstein, M.; Colby, R. H. *Macromolecules* **1991**, *24*, 4701–4707.
(27) Rubinstein, M.; Colby, R. H. *Polymer Physics*; Oxford University Press: New York, 2003.
(28) Langley, N. R. *Macromolecules* **1968**, *1*, 348–352.
(29) Alberty, R. A.; Silbey, R. J. *Physical Chemistry*; John Wiley & Sons, Inc.: New York, 2003.
(30) Bell, G. I. *Science* **1978**, *200*, 618–627.
(31) Kersey, F. R.; Yount, W. C.; Craig, S. L. *J. Am. Chem. Soc.* **2006**, *128*, 3886–3887.
(32) Kersey, F. R.; Loveless, D. M.; Craig, S. L. *J. R. Soc. Interface* **2007**, *4*, 373–380.
(33) Tennyson, A. G.; Wiggins, K. M.; Bielawski, C. W. *J. Am. Chem. Soc.* **2010**, *132*, 16631–16636.
(34) Rubinstein, M.; Semenov, A. N. *Macromolecules* **2001**, *34*, 1058–1068.
(35) Milner, S. T.; McLeish, T. C. B. *Phys. Rev. Lett.* **1998**, *81*, 725–728.
(36) Pattamaprom, C.; Larson, R. G. *Macromolecules* **2001**, *34*, 5229–5237.
(37) Larson, R. G.; Sridhar, T.; Leal, L. G.; McKinley, G. H.; Likhtman, A. E.; McLeish, T. C. B. *J. Rheol.* **2003**, *47*, 809–818.
(38) Hong, P. D.; Chou, C. M.; He, C. H. *Polymer* **2001**, *42*, 6105–6112.
(39) Liu, Y. G.; Jun, Y. G.; Steinberg, V. *J. Rheol.* **2009**, *53*, 1069–1085.